Published in final edited form as:
Microsc Microanal. 2012 June ; 18(3): 445–452. doi:10.1017/S1431927612000190.

Acute Lung Injury Induced by Staphylococcal enterotoxin B: Disruption of Terminal Vessels as a Mechanism of Induction of Vascular Leak

Ali Imran Saeed[#1,‡], **Sadiye Amcaoglu Rieder**[#2,¶], **Robert L. Price**[3], **James Barker**[1,§], **Prakash Nagarkatti**[2], and **Mitzi Nagarkatti**[2,*]

[1]Division of Pulmonology, Department of Internal Medicine, University of South Carolina School of Medicine, Columbia, SC 29209, USA

[2]Department of Pathology, Microbiology and Immunology, University of South Carolina School of Medicine, Columbia, SC 29209, USA

[3]Department of Cell Biology and Anatomy, University of South Carolina School of Medicine, Columbia, SC 29209, USA

[#] These authors contributed equally to this work.

Abstract

The current hypothesis of alveolar capillary membrane dysfunction fails to completely explain the severe and persistent leak of protein-rich fluid into the pulmonary interstitium, seen in the exudative phase of acute lung injury (ALI). The presence of intact red blood cells in the pulmonary interstitium may suggest mechanical failure of pulmonary arterioles and venules. These studies involved the pathological and ultrastructural evaluation of the pulmonary vasculature in Staphylococcal enterotoxin B(SEB)-induced ALI. Administration of SEB resulted in a significant increase in the protein concentration of bronchoalveolar lavage fluid and vascular leak in SEB-exposed mice compared to vehicle-treated mice. *In vivo* imaging of mice demonstrated the pulmonary edema and leakage in the lungs of SEB-administered mice. The histopathological studies showed intense clustering of inflammatory cells around the alveolar capillaries with subtle changes in architecture. Electron microscopy studies further confirmed the diffuse damage and disruption in the muscularis layer of the terminal vessels. Cell death in the endothelial cells of the terminal vessels was confirmed with TUNEL staining. In this study, we demonstrated that in addition to failure of the alveolar capillary membrane, disruption of the pulmonary arterioles and venules may explain the persistent and severe interstitial and alveolar edema.

[*]*Corresponding author*. Mitzi.Nagarkatti@uscmed.sc.edu.
[‡]Current address: Department of Pulmonary Critical Care and Sleep Medicine, MSC10-5550, University of New Mexico, Albuquerque, NM 87131, USA
[¶]Current address: Laboratory of Immunology, Cellular Immunology Section, National Institutes of Health, Bethesda, MD 20892, USA
[§]Current address: Department of Pulmonary Critical Care and Sleep Medicine, Scott and White Health System, Texas A&M HCS, Temple, TX 76508, USA

Keywords

electron microscopy; pulmonary vascular leak; acute respiratory distress syndrome; acute lung injury

Introduction

Acute lung injury (ALI) remains an important problem worldwide. In the United States, there are about 190,600 cases each year with approximately 70,000 deaths and 3.6 million hospital days (Maybauer et al., 2006). ALI is characterized by hypoxemic respiratory failure, noncardiogenic edema, and elevation in pulmonary vascular pressure (Bernard et al., 1994; Artigas et al., 1998). The management of ALI centers around three main therapies: supportive care, mechanical ventilation, and administration of pharmacological agents such as immunosuppressive drugs (Diaz et al., 2010). Recent advances in low-tidal volume ventilation have reduced the mortality rates down to 30–40%. However, this lethal condition remains a serious health problem in intensive care units all over the world (Wheeler & Bernard, 2007). There are three main phases of ALI, and the clinical course of disease is variable within patients. During the acute phase (also known as the exudative phase), neutrophils infiltrate the alveolar space as well as the interstitium causing extensive damage to the endothelial cells. In the fibroproliferative phase, hyaline membranes thicken thereby resulting in interstitial fibrosis. The final stage, which is the resolution phase, involves removal of apoptotic cells as well as the protein-rich exudates, and remodeling of the lung matrix (Tsushima et al., 2009).

Diffuse alveolar damage is the main histopathological feature in early ALI (Beasley, 2010). The ultrastructural changes seen in ALI include endothelial cell swelling, widening of interendothelial gap junctions, and increased number of pinocytotic vesicles (Maniatis et al., 2008). In addition, intravascular fibrin formation, endothelial cell necrosis, and basement membrane disruption are frequently noted (Lucas et al., 2009). The pulmonary arterioles and venules are thought to have a muscular barrier and are considered resistant to mechanical disruption during ALI.

In this study, we used a superantigen, Staphylococcal enterotoxin B(SEB), to induce a murine model of ALI. As a superantigen, SEB activates a higher proportion of the T cells compared with a conventional antigen (Fraser & Proft, 2008). Especially, T cells with specific T cell receptors, such as Vβ8 or Vβ2, are activated resulting in the recruitment and activation of other immune cells such as macrophages and natural killer cells (Henghold, 2004). Secretion of potent inflammatory cytokines and cytotoxic killing of endothelial cells result in vascular permeability, therefore causing respiratory failure (Neumann et al., 1997).

Over the past decades, research in ALI demonstrated that the extent of interstitial edema is disproportionate to the mild changes seen in the endothelial cells of the capillaries (Tomashefski, 2000). In this study, we hypothesized that the pulmonary arterioles and venules, collectively named terminal vessels, also undergo stress failure in SEB-induced inflammation. The pressure drop in the distal capillaries caused by the failure in high-

pressure arterioles may allow capillaries to remodel, thus explaining the subtle changes seen in the capillary bed.

Materials and Methods

Reagents

SEB was purchased from Toxin Technology Inc. (Sarasota, FL, USA). The purity of the SEB was 95% as determined by SDS-PAGE.

Animals

Adult female mice on the C57BL/6 background were purchased from the National Cancer Institute (Bethesda, MD, USA). Mice used in this study were at the age of 7–8 weeks. The colony was maintained at the animal facility of the School of Medicine, University of South Carolina (Columbia, SC, USA). All procedures were approved by the University of South Carolina Institutional Animal Care and Use Committee (Columbia, SC, USA).

Murine Model of Acute Lung Injury

To induce ALI in mice, SEB (50 μg/mouse) was administered through the intranasal route in 50 μL of phosphate buffered saline (PBS). Control mice received 50 μL of sterile PBS through the intranasal route. The end point for all the experiments was 48 h after superantigen administration (Rieder et al., 2011).

Evans Blue Extravasation

At the 48 h time point, groups of four mice were injected with 1% Evans blue prepared in PBS (100 μL/mouse intravenously). Two hours later, the mice were exsanguinated and perfused through the heart with heparinized PBS. After complete removal of blood, the lungs were excised out and placed in formamide. The tissues were incubated at 37°C for 24 h and the absorbance of formamide was measured at 620 nm.

Measuring Protein Concentration in Bronchoalveolar Fluid

To obtain bronchoalveolar fluid (BALF), the trachea were tied with surgical sutures, and the whole set of lungs was removed. Then, 1 mL of sterile PBS was pushed through the whole lungs several times, and the tissue was minced with a scalpel to recover optimum amounts of lavage fluid. The BALF for each mouse ($n = 4$) was collected, centrifuged, and the supernatants were collected for analysis. A Bradford protein assay was used to measure protein concentration.

In Vivo Imaging of Acute Lung Injury

ALI was induced as described above, after 48 h of SEB administration, 100 μL FITC-conjugated polystyrene beads (100 nm, PolySciences, Inc., Warrington, PA, USA) were injected through the retro-orbital vein into PBS ($n = 3$) and SEB-exposed mice ($n = 3$). The mice were imaged with the IVIS Spectrum (Caliper Life Sciences, Hopkinton, MA, USA) *in vivo* imaging system 6 h after fluorescent-bead injection.

Hematoxylin and Eosin Staining

The lungs were harvested from the control as well as SEB-exposed mice (n = 3) 48 h after toxin administration. The specimens were immediately placed in 10% formalin and fixed for 24 h. Using a microtome, 6 μm sections were obtained from the paraffin embedded tissue and then placed on glass slides. For staining, slides were placed in xylene and alcohol gradients (100%, 95%, and 80%, respectively) so as to remove the paraffin. These slides were then placed in hematoxylin solution for 7 min, rinsed with water, and stained with eosin for 2 min. Next, the slides were once again placed in alcohol gradients (95% and 100%, respectively) and cleared with xylene before coverslipping. A Nikon E600 with QCapture software was used to obtain images at 4×, 20×, and 40×.

Electron Microscopy

The lungs were harvested from control (n = 5) and SEB-exposed mice (n = 5), 48 h after toxin administration, and stained as reported previously (Rafi et al., 1998; Rafi-Janajreh et al., 1999). Briefly, small pieces of tissue were excised from each specimen and were immediately fixed in 2% glutaraldehyde/1% paraformaldehyde/0.1 M Na cacodylate. The tissues were rinsed with 0.1 M Na cacodylate and fixed once again with 1% osmium tetroxide. Next, the samples were rinsed with water and dehydrated by rinsing the samples in 25%, 50%, 75%, and 95% ethanol, respectively. These samples were then placed in 100% acetone as the transitional solvent and infiltrated in PolyBed 812. Next, the tissues were embedded in BEEM® capsules (BEEM, Inc., West Chester, PA, USA); the sections were cut with a microtome and placed on the grids. The grids were then stained with uranyl acetate, followed by exposure to sodium hydroxide pellets and lead staining. A JEOL 200CX transmission electron microscope (JEOL, Ltd., Tokyo, Japan) and Advanced Microscopy Techniques Corp. (Woburn, MA, USA) camera and software were used to obtain the images. The images were obtained at 3,700×, 7,000×, 10,000×, and 20,000×.

TUNEL Staining

The lungs were harvested from the control (n = 4) as well as SEB-exposed mice (n = 4), 48 h after toxin administration. The specimens were immediately placed in 10% formalin and fixed for 24 h. Using a microtome, 6 μm sections were obtained from the paraffin embedded tissue and then placed on glass slides. Lung sections were stained with the Dead End Colorometric TUNEL system (Promega, Madison, WI) according to the company's instructions. The apoptotic cells appear dark brown, while healthy cells have dark blue nuclei. The slides were analyzed with a light microscope, and the pictures were taken at 100×. Hematoxylin was used as a counterstain

Statistics

Data shown in this article represent at least three independent experiments. The means ± standard error of the mean are shown for experiments that are applicable. The statistical difference was calculated with the Student's t-test and the p value of ≤0.05 was considered to be statistically significant.

Results

Administration of SEB Results in Vascular Leak and Acute Lung Injury

During the acute phase of ALI, the endothelial cells of the capillaries as well as the epithelial cells of the alveolar walls undergo cell death, resulting in the leakage of protein-rich fluid into the alveolar space and the interstitium. We measured the protein concentration of the BALF, 48 h after SEB administration, and demonstrated that SEB-treated mice had significantly higher protein concentration in their lungs compared to PBS-treated mice (Fig. 1A). Evans blue extravasation studies further confirmed the extensive damage in the lungs of mice because the dye concentration was significantly higher in the BALF of SEB-administered mice compared to PBS-treated mice (Fig. 1B). In addition, we employed a novel method of *in vivo* imaging to demonstrate edema in this murine model of ALI. We showed that injection of fluorescent beads into the PBS-treated mice did not result in edema because the capillaries and the terminal vessels were intact. However, the fluorescent beads extravasated into the alveolar space and the interstitium of the lungs in SEB mice because the intensity of the fluorescent signal was increased during imaging (Fig. 1C).

SEB Administration Leads to Massive Infiltration of Lymphocytes into the Lungs

Analysis of hematoxylin and eosin (H&E) sections at low magnification demonstrated the clustering of inflammatory cells within the interstitium of the lungs, while the sections from control mice showed normal lung histopathology (Fig. 2A). On higher magnification, the infiltration of lymphocytes around capillaries (red arrows) was evident. More importantly, there was intense clustering (10 ± 5 rings of cells) of inflammatory cells around the terminal vessels (black arrows) in the SEB-treated group (Fig. 2B). Close examination of the terminal vessels also demonstrated that the inflammatory cells have eroded through the muscular layer, demonstrating the destruction of these terminal vessels (depicted by black arrows) (Fig. 2C). Mice that were exposed to intranasal PBS administration showed normal histopathology of terminal vessels.

Exposure to SEB Causes Subtle Ultrastructural Changes in the Capillaries, While It Causes Failure in Terminal Vessels during the Acute Phase of ALI

We studied the ultrastructure of the lung tissue after SEB administration. The sections were examined to determine the areas under stress. Figure 3A shows examples of the normal architecture of capillaries, white blood cells, and endothelial cells. The close examination of the capillaries in SEB mice showed necrotic endothelial cells (Fig. 3B). There were multiple fields showing complete replacement of lung architecture with clusters of inflammatory cells in SEB sections. However, all the capillaries maintained their architecture (Fig. 3C) even if there was intense clustering of inflammatory cells (Fig. 3D). The alveolar sacs and interstitial space in areas of preserved architecture showed cellular debris, intact red blood cells (RBCs), fibrinous bands, and highly active inflammatory cells (Fig. 3D).

We further examined the ultrastructure of terminal vessels upon SEB administration. Figure 3E represents an electron microscopy (EM) section from PBS-administered mice and shows the normal architecture of a vessel with a thick layer of smooth muscle layer indicated by arrows. The examination of the SEB-exposed sections showed intense clustering of

inflammatory cells around the terminal vessels with thinning of the smooth muscle layer (Fig. 3F). The stress failure in terminal vessels was also evident in the sections from SEB-exposed mice, where the smooth muscle layer was compromised at certain locations pointed-out by the arrows (Figs. 3G, 3H). Several EM fields revealed stress failure of the terminal vessels with actual gap formation, in which the muscularis layer was completely destroyed (Figs. 3J, 3L). In some sections, the terminal vessels were visible; however, the surrounding smooth muscle layer was absent in its entirety (Fig. 3M). Finally, the damage to the terminal vessels was confirmed because a RBC was being "squeezed out" into the alveolar space (Fig. 3N). Figures 3I and 3K were sections from PBS-exposed mice to show the normal architecture of the terminal vessels.

SEB Administration Causes Cell Death in the Endothelial Cells of the Terminal Vessels

It is known that endothelial cell death in the capillaries is the main culprit of vascular leak during ALI. We wanted to determine whether SEB administration also resulted in cell death in the endothelial cells of the terminal vessels. We demonstrated that the endothelial cells in PBS-exposed mice were healthy because the nuclei of the cells stained dark blue (Fig. 4A). The sections from SEB-exposed mice demonstrated extensive cell death by apoptosis in the endothelial cells of the terminal vessels as shown by black arrows (Fig. 4B). These studies show that cell death may occur both through apoptosis as well as necrosis as observed in ultra-structural studies.

Discussion

The hallmark of ALI is considered to be the opening of endothelial gap junctions and leakage of protein rich edema fluid into the alveolar interstitial space. This hypothesis fails to explain several important points in disease pathology. First, the abundant presence of intact RBCs should reflect the stress damage on the cell wall of the endothelial cells. However, subtle changes in capillaries are noted during ALI. In addition, not all patients with inflammatory, chemical, or immune insults progress into the catastrophic end point of lung fibrosis. Finally, it is a diagnostic puzzle as to why conservative fluid administration and specific ventilator therapy is not consistently effective in disease treatment.

In this study, we challenged the argument that the terminal vessels (pulmonary arterioles and venules) are relatively resistant to stress failure and considered almost indestructible during ALI. We demonstrated the failure of terminal vessels by ultrastructural studies and put forward the suggestion that it may be due to the pressure drop hypothesis, which is based on the pressure and flow principle. Once the high-pressure terminal arterioles undergo stress failure, the distal capillaries experience a drop in pressure. This allows capillaries to adapt and maintain their structure, making the failure in terminal vessels the primary source of edema.

ALI was induced in mice with administration of SEB (50 μg/mouse) through the intranasal route. In our recent studies, we have used 12.5, 25, and 50 μg doses of SEB intranasally, which is the prevalent mode of exposure to this toxin and studied vascular leak at 24, 48, and 72 h (Rieder et al., 2011). Our studies demonstrated that a 50 μg dose of SEB caused the highest amount of vascular leak at 48 h, which was mediated by natural killer-T cells. In our

initial studies, we also performed intraperitoneal (i.p.) administration of SEB, and this led to lower levels of vascular leak in the lungs. This may be because i.p. administration is a systemic challenge versus the direct administration of toxin into the lungs via intranasal administration.

There are several ways by which ALI is quantitated including determining wet/dry weight ratios of the lungs, estimation of protein concentration in BALF, as well as Evans blue extravasation assays (Rafi et al., 1998; Rafi-Janajreh et al., 1999; Teke et al., 2011). Using the latter two methodologies, we demonstrated that after 48 h the protein rich exudate is profusely present in the BALF of SEB-treated mice. In addition, the vascular leak in SEB mice was significantly increased compared to PBS-treated control mice. Neumann et al. (1997) previously performed studies following i.p. administration of SEB that resulted in ALI. This study also confirmed the involvement of granulocytes, macrophages, and natural killer cells in disease pathogenesis, which are the same cells responsible for ALI in human cases (Tsushima et al., 2009). The study also demonstrated the predominant role played by neutrophils in mediating the injury, which was attributed to oxidant production. Furthermore, the report addressed the role of adhesion molecules such as VCAM-1 and ICAM-1 in the lungs of SEB-treated mice, albeit it is not clear precisely which cells express these. In contrast, our studies examined the effects using a clinically relevant mode of exposure, namely intranasal route of administration of SEB. Our studies have also demonstrated the increased infiltration with inflammatory cells following SEB treatment, and in addition, we have found that the mechanism of endothelial cell damage is through induction of apoptosis as well as necrosis. While apoptosis and necrosis were considered as distinct pathways in cell death, it is now well established that molecules involved in apoptosis may also participate in induction of necrosis (Green et al., 2011).

On the other hand, studies by Mattix et al. (1995) have examined the pulmonary lesions in rhesus monkeys following administration of aerosolized SEB, although their work was mainly restricted to ultrastructural examination of the lungs. While these studies also concluded the presence of lung-infiltrating mononuclear cells, the mechanism by which the lung damage occurs was not determined. Campbell et al. (1997) have demonstrated the direct cytotoxic activity of SEB using exclusively pulmonary artery endothelial cells *in vitro*. They have also undertaken studies to demonstrate the downstream signaling pathways leading to endothelial cell (EC) injury by determining the protein tyrosine kinase activity using these cells *in vitro*. Thus, our studies are a significant advance in the field in that we have demonstrated that the vascular leak that is seen following SEB administration may be due to damage in endothelial cells in the terminal vessels rather than exclusively through disruption of endothelial gap junctions in capillaries, which is the commonly held view.

We also performed *in vivo* imaging with fluorescent beads in PBS- and SEB-treated mice, and clearly demonstrated the edema in our murine model. H&E staining also showed clustering of inflammatory cells around the capillaries and the terminal vessels. It is known that the animal models of acute lung injury have limitations. However, the SEB-induced model of ALI has many of the same pathophysiological features of the human condition (Matute-Bello et al., 2008).

In this article, we compared the ultrastructural changes seen in the capillaries versus the terminal vessels during ALI. It is already established that the endothelial cells of the capillaries undergo mechanical failure, resulting in edema. As described earlier, our ultrastructural studies also demonstrate endothelial cell necrosis and intense clustering of inflammatory cells around the capillaries with subtle changes in architecture. Comparatively, intense clustering of inflammatory cells was also noticed around the terminal vessels with patchy areas of thinning vessel wall in SEB-treated mice. In several EM fields, the vessel wall was completely destroyed with RBC being squeezed out into the interstitium. Other studies have described the damage to glomerular basement membrane during sporadic hematuria (Collar et al., 2001; Liapis et al., 2002). In these studies, one observation was the dumbbell shape of the RBC as it squeezed out into the Bowman's space. Interestingly, in our studies, we also noticed the dumbbell shape of the RBC as it was going through the damaged terminal vessel wall, confirming the mechanical failure in these vessels.

It is known that post-capillary venules are the major sites of protein-rich plasma leakage during asthma, resulting in airway submucosal and mucosal edema (Persson, 1986). It has also been demonstrated that inflammatory stimuli such as bradykinin, substance P, or formaldehyde gas administration can result in the leaking of plasma fluid in rat tracheal venules (McDonald, 1994; Baffert et al., 2006). These studies demonstrate the capability of terminal vessels, such as venules, to undergo mechanical failure during inflammation. Even though asthma consists of chronic inflammation, damage to the terminal vessels can also be achieved during acute lung inflammation. The current hypothesis of ALI is centered on alveolar capillary membrane failure. Our studies are novel in that they provide insights into understanding the exudative phase, which points to the fact that in addition to the presence of leak through gap junctions, the severe and persistent pulmonary edema may be due to mechanical disruption of terminal vessels. This is supported indirectly by clinical evidence in that the mortality and morbidity remains high. Clinically, the controversial role of steroids in acute respiratory distress syndrome may also be due to this phenomenon (Peter et al., 2007).

In conclusion, it is possible that the exudative phase of ALI consists of two distinct mechanisms, which include damage to the capillaries as well as the mechanical failure of the terminal vessels. This study sheds new light on the pathomechanism of ALI and explains yet another aspect of the biomechanism that may aid in generating better treatment options.

Acknowledgments

The authors gratefully thank Dr. Guilermo A. Herrera, Deputy Director, Bostwick Labs, Tempe, AZ for assistance in the ultrastructural evaluation of the data.

REFERENCES

Artigas A, Bernard GR, Carlet J, Dreyfuss D, Gattinoni L, Hudson L, Lamy M, Marini JJ, Matthay MA, Pinsky MR, Spragg R, Suter PM. The American-European Consensus Conference on ARDS, part 2: Ventilatory, pharmacologic, supportive therapy, study design strategies, and issues related to recovery and remodeling. Acute respiratory distress syndrome. Am J Respir Crit Care Med. 1998; 157:1332–1347. [PubMed: 9563759]

Baffert F, Le T, Thurston G, McDonald DM. Angiopoietin-1 decreases plasma leakage by reducing number and size of endothelial gaps in venules. Am J Physiol Heart Circ Physiol. 2006; 290:107–118.

Beasley MB. The pathologist's approach to acute lung injury. Arch Pathol Lab Med. 2010; 134:719–727. [PubMed: 20441502]

Bernard GR, Artigas A, Brigham KL, Carlet J, Falke K, Hudson L, Lamy M, Legall JR, Morris A, Spragg R. The American-European Consensus Conference on ARDS. Definitions, mechanisms, relevant outcomes, and clinical trial coordination. Am J Respir Crit Care Med. 1994; 149:818–824. [PubMed: 7509706]

Campbell WN, Fitzpatrick M, Ding X, Jett M, Gemski P, Goldblum SE. SEB is cytotoxic and alters EC barrier function through protein tyrosine phosphorylation in vitro. Am J Physiol. 1997; 273:31–33.

Collar JE, Ladva S, Cairns TD, Cattell V. Red cell traverse through thin glomerular basement membranes. Kidney Int. 2001; 59:2069–2072. [PubMed: 11380808]

Diaz JV, Brower R, Calfee CS, Matthay MA. Therapeutic strategies for severe acute lung injury. Crit Care Med. 2010; 38:1644–1650. [PubMed: 20562704]

Fraser JD, Proft T. The bacterial superantigen and superantigen-like proteins. Immunol Rev. 2008; 225:226–243. [PubMed: 18837785]

Green DR, Oberst A, Dillon CP, Weinlich R, Salvesen GS. RIPK-dependent necrosis and its regulation by caspases: A mystery in five acts. Mol Cell. 2011; 44:9–16. [PubMed: 21981915]

Henghold WB 2nd. Other biologic toxin bioweapons: Ricin, staphylococcal enterotoxin B, and trichothecene mycotoxins. Dermatol Clin. 2004; 22:257–262. [PubMed: 15207307]

Liapis H, Foster K, Miner JH. Red cell traverse through thin glomerular basement membrane. Kidney Int. 2002; 61:762–763. [PubMed: 11849422]

Lucas R, Verin AD, Black SM, Catravas JD. Regulators of endothelial and epithelial barrier integrity and function in acute lung injury. Biochem Pharmacol. 2009; 77:1763–1772. [PubMed: 19428331]

Maniatis NA, Kotanidou A, Catravas JD, Orfanos SE. Endothelial pathomechanisms in acute lung injury. Vascul Pharmacol. 2008; 49:119–133. [PubMed: 18722553]

Mattix ME, Hunt RE, Wilhelmsen CL, Johnson AJ, Baze WB. Aerosolized staphylococcal enterotoxin B-induced pulmonary lesions in rhesus monkeys (Macaca mulatta). Toxicol Pathol. 1995; 23:262–268. [PubMed: 7659951]

Matute-Bello G, Frevert CW, Martin TR. Animal models of acute lung injury. Am J Physiol Lung Cell Mol Physiol. 2008; 295:379–399.

Maybauer MO, Maybauer DM, Herndon DN. Incidence and outcomes of acute lung injury. N Engl J Med. 2006; 354:416–417. [PubMed: 16444810]

McDonald DM. Endothelial gaps and permeability of venules in rat tracheas exposed to inflammatory stimuli. Am J Physiol. 1994; 266:61–83.

Neumann B, Engelhardt B, Wagner H, Holzmann B. Induction of acute inflammatory lung injury by Staphylococcal enterotoxin B. J Immunol. 1997; 158:1862–1871. [PubMed: 9029127]

Persson CC. The role of microvascular permeability in the pathogenesis of asthma. Eur J Respir Dis Suppl. 1986; 144:190–216. [PubMed: 3462024]

Peter JV, John P, Graham PL, Moran JL, George IA, Bersten A. Corticosteroids in the prevention and treatment of acute respiratory distress syndrome (ARDS) in adults: Meta-analysis. BMJ. 2007; 336:1006–1009. [PubMed: 18434379]

Rafi AQ, Zeytun A, Bradley MJ, Sponenberg DP, Grayson RL, Nagarkatti M, Nagarkatti PS. Evidence for the involvement of Fas ligand and perforin in the induction of vascular leak syndrome. J Immunol. 1998; 161:3077–3086. [PubMed: 9743374]

Rafi-Janajreh AQ, Chen D, Schmits R, Mak TW, Grayson RL, Sponenberg DP, Nagarkatti M, Nagarkatti PS. Evidence for the involvement of CD44 in endothelial cell injury and induction of vascular leak syndrome by IL-2. J Immunol. 1999; 163:1619–1627. [PubMed: 10415067]

Rieder SA, Nagarkatti P, Nagarkatti M. Cd1d-independent activation of invariant natural killer T cells by Staphylococcal enterotoxin B through major histocompatibility complex class II/T cell receptor interaction results in acute lung injury. Infect Immun. 2011; 79:3141–3148. [PubMed: 21628519]

Teke Z, Adali F, Kelten EC, Enli Y, Sackan KG, Karaman K, Akbulut M, Goksin I. Mannitol attenuates acute lung injury induced by infrarenal aortic occlusion-reperfusion in rats. Surg Today. 2011; 41:955–965. [PubMed: 21748612]

Tomashefski JF Jr. Pulmonary pathology of acute respiratory distress syndrome. Clin Chest Med. 2000; 21:435–466. [PubMed: 11019719]

Tsushima K, King LS, Aggarwal NR, De Gorordo A, D'Alessio FR, Kubo K. Acute lung injury review. Intern Med. 2009; 48:621–630. [PubMed: 19420806]

Wheeler AP, Bernard GR. Acute lung injury and the acute respiratory distress syndrome: A clinical review. Lancet. 2007; 369:1553–1564. [PubMed: 17482987]

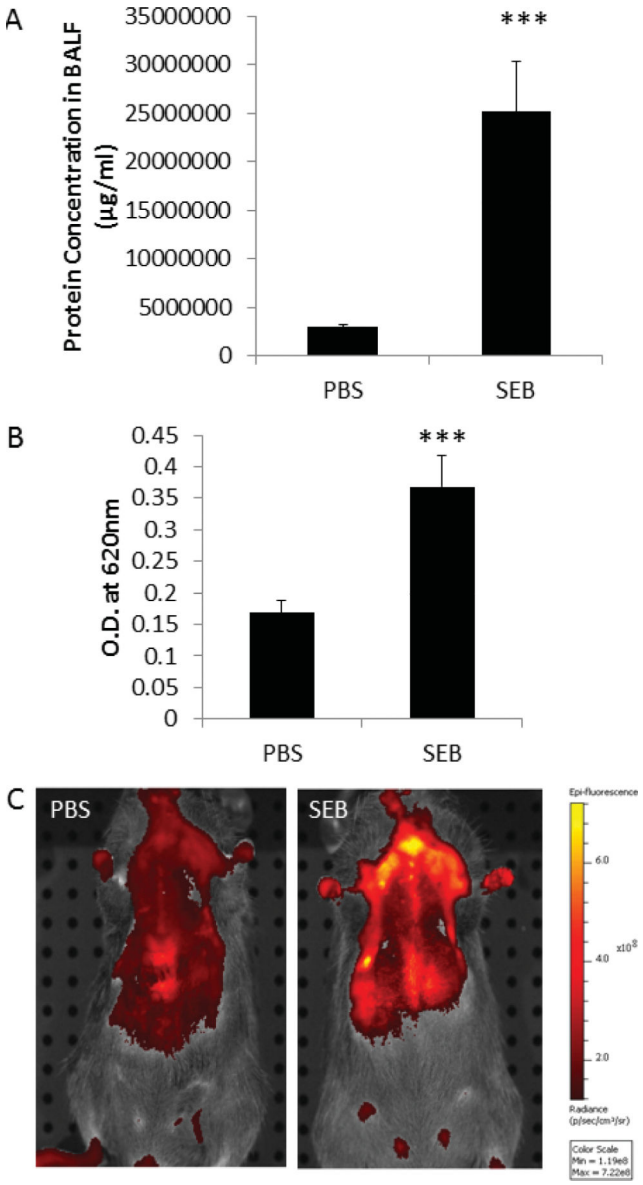

Figure 1.

Administration of SEB results in vascular leak and acute lung injury. SEB (50 μg/mouse) was administered through the intranasal route, and PBS was used as control. The mice were exsanguinated 48 h later to study acute lung injury. **A:** Protein concentration in the BALF from PBS and SEB-treated mice. **B:** Evans blue measurement in the lungs of PBS and SEB mice. **C:** *In vivo* imaging of edema in the lungs of PBS and SEB mice (***p , 0.001).

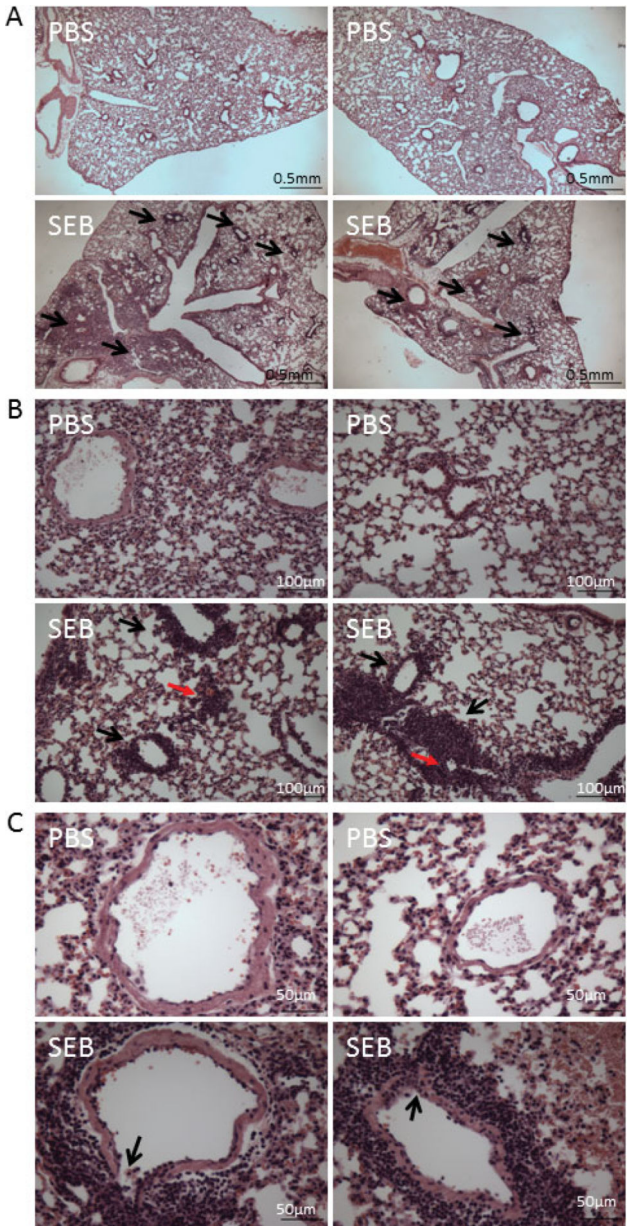

Figure 2.

SEB administration leads to a massive infiltration of leukocytes into the lungs. ALI was induced as described in the methods, and 48 h later, the lungs were excised out for H&E staining. **A:** The pictures were taken at 4×. The black arrows indicate areas with intense clustering of inflammatory cells in SEB-treated mice. **B:** The pictures were taken at 20×. The black arrow indicates the presence of inflammatory cells around the terminal vessels, while red arrows show infiltration around capillaries. **C:** The pictures were taken at 40×. The arrow indicates the destruction of the terminal vessel by the inflammatory cells. There is significant perivascular clustering of inflammatory cells in SEB-treated mice with a mean of 10 ± 5 rings of inflammatory cells around the vessels when compared to none in controls.

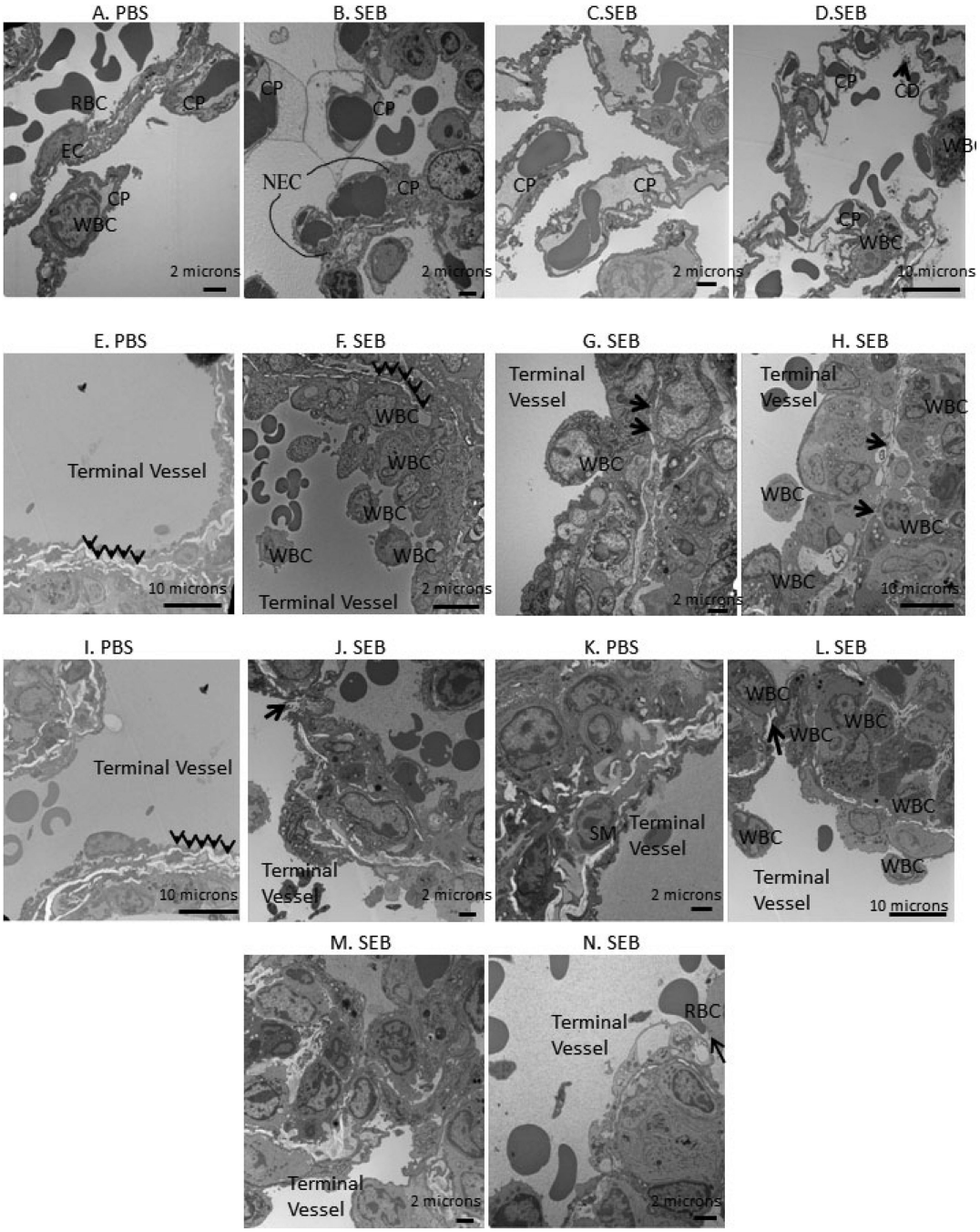

Figure 3.

Exposure to SEB causes subtle ultrastructural changes in the capillaries during ALI. **A:** The normal architecture of a capillary in PBS exposed mice with intact basal lamina. **B–D:** Ultrastuctural studies following SEB treatment. **B:** Presence of intact RBCs in the interstitium. **C:** Severe clustering of inflammatory cells around the capillaries. **D:** Cellular debris and intact RBCs in the interstitium of the lungs. Exposure to SEB causes failure in terminal vessels during the acute phase of ALI. **E:** The terminal vessel architecture is well preserved in PBS-treated mice with intact smooth muscle cell layer. **F:** The clustering of

inflammatory cells around a terminal vessel with thinning smooth muscle layer. **G,H:** Thinning and stress failure in the terminal vessel shown by black arrows. **I,K:** The normal architecture of a terminal vessel in PBS-exposed mice. **J,L:** Gap formation in the terminal vessel indicated by black arrows. **M:** Intense clustering around the terminal vessel and the complete disruption in the smooth muscle layer architecture. **N:** A RBC being squeezed out into the interstitium with intense clustering around the terminal vessel. Abbreviations: RBC, red blood cell; EC, endothelial cell; CP, capillary; CD, cellular debris; WBC, white blood cell; NEC, necrotic endothelial cell.

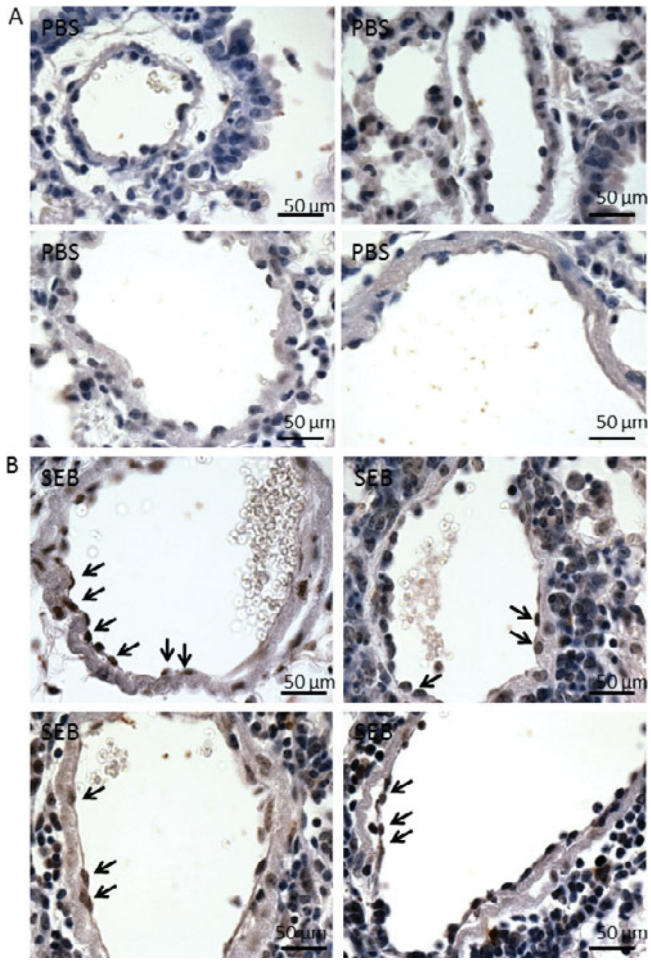

Figure 4.

SEB administration causes cell death in the endothelial cells of the terminal vessels. **A:** In PBS-exposed mice, the endothelial cells that line the lumen side of terminal vessels appear healthy as indicated by dark blue staining in the nuclei. **B:** SEB administration induces cell death in the endothelial cells because the nuclei of some of the cells stain dark brown, indicative of DNA fragments (examples are shown with black arrows). SEB exposed mice had 3.75 ± 2.25 TUNEL positive endothelial cells on an average when compared to none in controls.